Effects of Temperature and Shape on the Tensile Behavior of Platinum Nanowires

S. J. A. Koh*, H. P. Lee, C. Lu and Q. H. Cheng

*Institute of High Performance Computing
1 Science Park Road, #01-01, The Capricorn, Singapore Science Park II, Singapore 117528, Singapore.
kohsj@ihpc.a-star.edu.sg

ABSTRACT

Molecular dynamics (MD) simulation was performed on an fcc solid platinum nanowire in this study. Infinite one-dimensional nanowires of circular and rectilinear cross sectional shapes were subjected to uniaxial tensile strain, and simulated at temperatures of 50K and 300K. The constitutive stress-strain response of the nanowire was investigated, the changes in crystal structure during axial deformation was studied and mechanical properties like first yield stress and strain, rupture strain, ductility and Young's modulus were deduced from the simulation statistics. It was observed that the nanowire with a rectilinear cross section generally exhibited greater ductility, with a correspondingly lower first yield stress and strain. The nanowire with a circular cross section displayed a higher tendency for the formation of a helical substructure during severe necking. These observations were more significant at the higher temperature of 300K. Young's modulus at nanoscale was also investigated.

Keywords: platinum nanowire, shape effect, temperature effect, molecular dynamics simulation, helical substructure.

1 OVERVIEW

Nanoscale research has flourished over the past decade. This was largely due to the overall enhanced mechanical, chemical, optical, electrical and magnetic properties of materials at characteristic sizes smaller than 100 nm [1]. The fabrication, characterization, experimentation and simulation of metallic nanomaterials had found much favor in nanoscale research during recent years. This could be attributed to its exceptionally high electrical conductivity, super-paramagnetic properties, superplasticity, high material strength, enhanced catalytic properties and high degree of biocompatibility at nanoscale.

Platinum was shown to have high resistance to corrosion, high ductility, low electrical resistance, high reactivity and is in relative abundance, as compared to other rare metals [2]. As such, platinum nanomaterials have been commonly used for catalysis, for opto-electronic purposes, for STM tips [3], as a superconductor, and as actuators [4] and very-high frequency (VHF) oscillators [5]. While ultrathin, single-walled platinum nanowires had been fabricated by Oshima *et. al.* [6], the mechanical behavior of such nanowires were scarcely reported [7,8]. Since platinum nanowires were currently used as AFM tips [3], actuators and VHF oscillators, detailed knowledge of its mechanical properties is essential.

This paper presents the MD simulation of a platinum nanowire under uniaxial tensile strain. A solid nanowire with an fcc crystal lattice atomic arrangement was simulated, using a stable crystal configuration which consists of 392 atoms. The crystal deformation behavior, constitutive response and mechanical properties were studied for infinite nanowires of circular and rectilinear cross sections. Thermal effects on the mechanical behavior were also investigated by performing the simulations at temperatures of 50K (the melting point of common gases like N_2 and O_2) and 300K (the standard laboratory temperature).

2 SIMULATION BRIEF

Classical MD simulation was performed on a 392-atom nanowire, with rectilinear and circular cross sections.

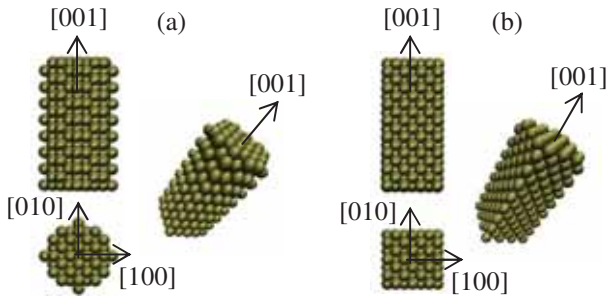

Figure 1: Platinum nanowire at initial stable configuration (a) circular cross section; (b) rectilinear cross section.

The circular cross section was obtained by building layers of atoms in an fcc lattice about the central [001] axis of the nanowire, which was terminated at the 8th nearest neighbor, giving a diameter of about 1.6 nm. The rectilinear section was obtained by repeated stacking of fcc unit cells in the [100] and [010] direction, terminated at the 6th unit cell in each direction, giving a square section of about 1.2 nm x 1.2 nm. 16 atomic layers in the [001] direction were simulated for both sections. Periodic boundary conditions

were applied in the [001] direction only, in order to simulate an infinite one-dimensional nanowire. Figure 1 shows the initial stable configuration of the platinum nanowires. The nanowire was stretched at a constant strain rate of 0.04% ps^{-1} in the [001] direction. The Berendsen thermostat [9] was used for temperature control by coupling the simulated system to an external heat bath, with a time constant of $\tau = 2.5$ ps. The simulation time-step was fixed at 1.0 fs (10^{-15} s). The nanowire was initially allowed to stabilize and relax to its equilibrium configuration at the specified temperature over 10^5 time-steps (100 ps). Subsequently, the nanowire was strained at a fixed strain increment in accordance to the specified strain rate. Each strain step was followed by 9999 relaxation time-steps, giving each strain interval as 10 ps. System properties were obtained from the statistics of the final 2000 time-steps. The strain rate was therefore given as:

$$\dot{\varepsilon}_{zz} = \frac{\Delta\varepsilon_{zz}}{S \cdot \Delta t} \tag{1}$$

where $\varepsilon_{zz} = \Delta L_z / L_z$, refers to the nominal strain and $\Delta\varepsilon$ is the strain increment. S refers to the total time-steps during each strain increment, which was fixed at 10^4, and $\Delta t = 1.0$ fs. Hence, the strain increment of $\Delta\varepsilon = 0.4\%$ will give the specified strain rate of 0.04% ps^{-1}.

The Finnis and Sinclair [10] pair functional interatomic potential was commonly used for the simulation of metallic bonding. In this simulation, the interatomic potential parametrized by Sutton and Chen [11] for fcc metals were used for platinum. The potential in terms of interatomic separation r_{ij}, is as follows:

$$E_{SC} = \varepsilon\left[\frac{1}{2}\sum_{i=1}^{N}\sum_{\substack{j=1 \\ (j\neq i)}}^{N}\phi(r_{ij}) - c\sum_{i=1}^{N}\sqrt{s_i}\right] \tag{2a}$$

and

$$\phi(r_{ij}) = \left(\frac{a}{r_{ij}}\right)^n, \qquad s_i = \sum_{\substack{j=1 \\ (j\neq i)}}^{N}\left(\frac{a}{r_{ij}}\right)^m \tag{2b}$$

The constant a in equation (2b) is fixed to the crystal lattice parameter, and ε, c, m and n are optimized against the equilibrium crystal configuration, cohesive energy per atom, bulk modulus and elastic constants C_{11}, C_{12} and C_{44}. Table I shows the optimized parameters for platinum. It should be noted here that ε in equation (2) refers to the energy constant of the interatomic potential, which must not be confused with ε_{zz} (strain in the [001] direction).

Finally, the axial stress on the nanowire at strain state ε, was given as follows [12]:

$$\sigma_{zz}(\varepsilon) = \frac{1}{N}\sum_{i=1}^{N}\eta_{zz}^{i}(\varepsilon) \tag{3a}$$

where,

$$\eta_{zz}^{i}(\varepsilon) = \frac{1}{\Omega^i}\sum_{\substack{j=1 \\ (j\neq i)}}^{N}F_z^{ij}(\varepsilon)r_z^{ij}(\varepsilon) \tag{3b}$$

F_z^{ij} refers to the [001] vectoral component of the pair-wise interatomic force between atoms i and j, obtained from differentiating equation (2) with respect to r_{ij}. r_z^{ij} is the interatomic distance in the [001] direction between an atomic pair. Ω^i refers to the volume of atom i, which was assumed as a hard sphere in a closely-packed undeformed crystal structure. From equation (3), the stress-strain response of the nanowire could be obtained from the simulation statistics and mechanical properties could be deduced.

Functional Parameter	Optimized value
a (Å)	3.92
ε (meV)	19.833
c	34.408
m	8
n	10

Table 1: Optimized parameters for platinum.

3 SIMULATION RESULTS

A virtual experiment was conducted to study the deformation characteristics and mechanical properties of the platinum nanowire. In this experiment, each cross section simulated at the specified temperature was assigned 8 different potential cutoff values. This gave 8 samples for each section at each temperature, with a total of 32 simulations conducted for this investigation. The potential cutoffs were varied uniformly between 1.91a and 2.50a, where a is the equilibrium lattice parameter. The former was adopted by Finbow *et. al.* [7] in their simulations of a 360-atom platinum nanowire, and the latter is the conventional value used for Lennard Jones pair potential [13]. Visualization of trajectory files was done using the Visual Molecular Dynamics (VMD) software, which was developed by the Theoretical Physics Group of University of Illinois at Urbana Champaign (USA).

Figures 2 to 5 present the stress-strain response of both circular and rectilinear nanowires simulated at T = 50K and T = 300K. Figure 2 shows the circular nanowire simulated at T = 50K. Figure 3 shows the rectilinear nanowire simulated at T = 50K. Figures 4 and 5 show the simulation at T = 300K for the circular and rectilinear nanowires respectively. The atomic configuration for the solid stress-strain curves (with substructures, which will be mentioned later) at various strain states – represented by markers {1}

to {4} on the stress-strain plot – were shown alongside with the plots.

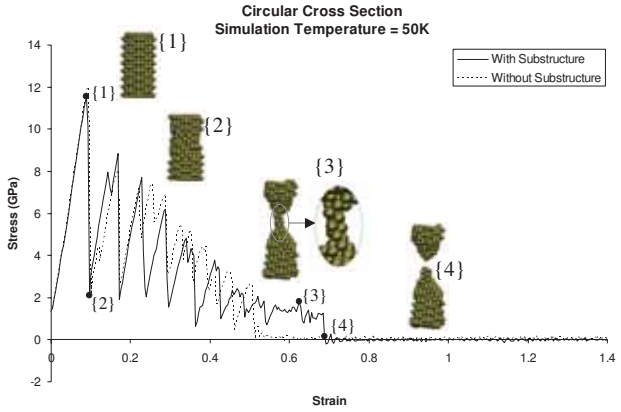

Figure 2: Stress-strain response of circular nanowire at T = 50K.

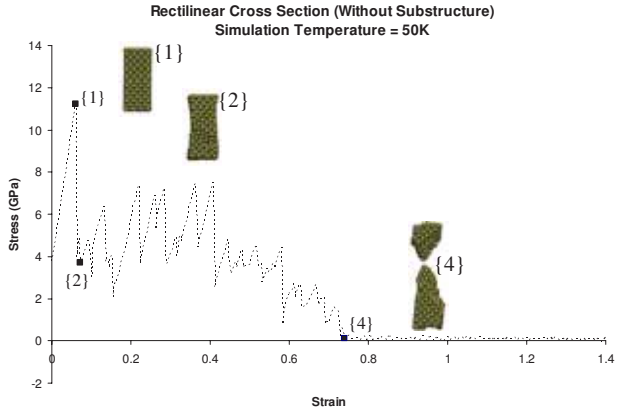

Figure 3: Stress-strain response of rectilinear nanowire at T = 50K.

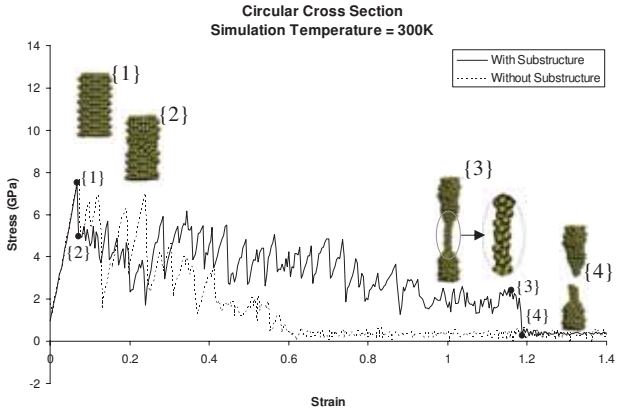

Figure 4: Stress-strain response of circular nanowire at T = 300K.

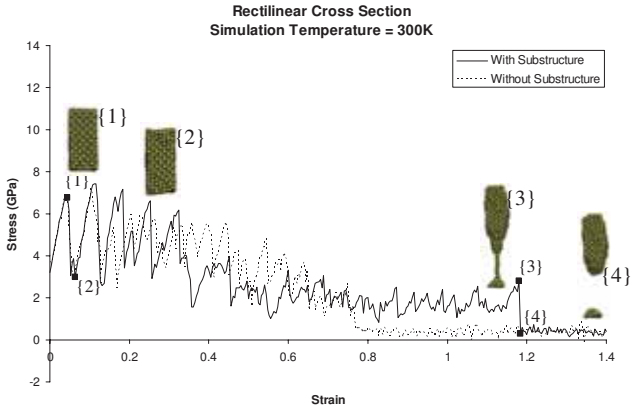

Figure 5: Stress-strain response of rectilinear nanowire at T = 300K.

From comparisons between Figures 2 and 4, and Figures 3 and 5, it was observed that first yield {1} occurred at a lower first yield stress (σ_{fy}) and first yield strain (ε_{fy}) for the nanowire at the higher temperature of T = 300K. At this strain state, there was an abrupt dislocation of the atomic positions from their equilibrium lattice positions, followed by an overall slippage along the (111) plane {2}. Due to the smaller Burger's vector for fcc crystals along the (111) plane, it was energetically more favorable for slippage to occur along this plane. From Figures 2 to 5, it was found that the first yield stress for the nanowire at T = 300K was about 35% to 40% lower than that at T = 50K, while the first yield strain was about 25% smaller. This was due to the higher atomic oscillation amplitude about their equilibrium lattice positions. This results in the destabilization of the crystal structure from its equilibrium configuration and encourages atoms to displace from its original lattice positions, and form slip planes. Furthermore, it was also observed that the rectilinear nanowire displayed marginally lower stress (3% - 10%) and a very much lower strain magnitude (30% - 35%) at first yield. This was a consequence of the shape effect whereby the rectilinear section has a higher degree of crystal order to be preserved as compared to that for the circular section. Due to the low coordination number for atoms located at the corners of the rectilinear section, the interatomic forces for these atoms was much larger than those located at the outermost layer of the circular section. This forces the corner line of atoms to collapse inwards into the internal bulk and therefore, resulting in slippage at a smaller first yield strain. Following the same argument, the large interatomic forces for the corner atoms of the rectilinear section would result in a slightly stiffer nanowire as compared to that of the circular section.

After the first yield, the nanowire undergoes a periodic recrystallization-yielding-relaxation process. This is a unique characteristic of crystalline materials at nanoscale. At this characteristic length scale, local atomic vibrations play a critical role in rearranging the crystal structure to a new equilibrium configuration after every planar slippage,

by the formation of a new layer of atoms. This periodic process continues until severe necking of the nanowire sets in, where amorphous deformation at the neck dominated the deformation behavior. It was observed that the nanowire ruptured {4} at a higher rupture strain (ε_{ru}) and hence, displayed higher ductility at T = 300K. This was due to the higher crystal disorder and higher amplitude of local atomic vibrations, which result in the preservation of significant interatomic attractive forces, leading to the formation of new equilibrium configurations even at high strain magnitudes. As a consequence of the higher vibration amplitude, the crystal structure slips and recrystallizes at a faster rate at T = 300K and therefore, smaller period of yielding was observed.

An interesting phenomenon was observed at strain state {3}, where formation of substructures was noted at the neck area. The formation of a double helical substructure was observed for the circular nanowire at both simulation temperatures and a single wire of platinum atoms evolved for the rectilinear nanowire at T = 300K. The presence of stable, single-walled helical platinum nanowires was discovered and fabricated by Oshima *et. al.* [6] at temperatures of 680K, and Finbow *et. al.* [7] reported the formation of a single wire of platinum atoms in their simulation. In our virtual experiment, substructure formation was only observed for cutoff values of 2.10a and 2.20a for the circular nanowire at T = 50K and T = 300K respectively, and 2.50a, for the rectilinear nanowire at T = 300K. None was observed for the rectilinear nanowire at T = 50K. The remaining cutoff values displayed necking and rupture of nanowire without formation of substructures. From the comparison of the stress-strain response of the nanowire with and without substructure formation, it was observed from Figures 2 to 5 that the former contributed significantly to the ductility of the nanowire. It was further observed that, the amount of increase in ductility was dependent on the type of substructure formed and total development length of the substructure before complete rupture occurs. From Figure 2, the approximate development length of the helical substructure was 7 Å and from Figure 4, the approximate development length was 20 Å, and Figure 5 showed the development of a 19 Å single wire of platinum atoms. From Figure 2, the formation of the 7 Å helical substructure resulted in a 36% increase in rupture strain magnitude. This was much smaller than the magnitude of increase observed in Figure 4, where the formation of a 20 Å helical substructure resulted in a 92% larger rupture strain. On the other hand, Figure 5 indicated that the formation of the single wire substructure resulted in a 54% increase in the rupture strain magnitude. This implies that the single wire substructure resulted in a much smaller increase in ductility as compared to the double-wire helical substructure of an approximately similar development length.

Young's modulus (E_{pt}) was obtained from the gradient of the stress-strain response before the first yield occurs. It was could be seen from Table 2 that the average Young's modulus from 8 simulated samples was about 5% higher for the rectilinear nanowire at T = 50K, and no significant difference was observed at T = 300K.

4 CONCLUSION

[a]Units in GPa
[b]Rupture strain with substructure formation

	Circular Section		Rectilinear Section	
	T=50K	T=300K	T=50K	T=300K
ε_{fy}	0.088	0.068	0.060	0.044
[a]σ_{fy}	11.53	7.52	11.23	6.77
ε_{ru}	0.512	0.620	0.740	0.772
[b]ε^{s}_{ru}	0.688	1.188	No Data	1.188
[a]E_{pt}	121.67	97.16	128.03	96.44

Table 2: Summary of mechanical properties.

Table 2 shows a summary of the mechanical properties obtained for the platinum nanowire in this investigation. These properties, together with the stress-strain response of the nanowire, could aid in future studies for the mechanical behavior of platinum nanowires.

REFERENCES

[1] J. L. Beeby, *Condensed Systems of Low Dimension, NATO Advanced Study Institute, Series B* **253**: Physics (New York: Plenum Press, 1991).
[2] R. B. Ross, *Metallic Materials Specification Handbook* (London: Chapman & Hall, 1992).
[3] N. Agraït, G. Rubion and S. Vieira, Phys. Rev. Lett. **74**, 3995 (1995).
[4] S. X. Lu and B. Panchapakesan, *IEEE, ICMENS 2004*, edited by IEEE Computer Society (Los Alamitos, California, 2004), p. 36.
[5] A. Husain *et. al.*, Appl. Phys. Lett. **83**, 1240 (2003).
[6] Y. Oshima *et. al.*, Phys. Rev. B **65**, 121401 (2002).
[7] G. M. Finbow, R. M. Lynden-Bell and I. R. McDonald, Mol. Phys. **92**, 705 (1997).
[8] Q. H. Cheng, H. P. Lee and C. Lu, Mol. Sim. (to be published).
[9] H. J. C. Berendsen *et. al.*, J. Chem. Phys. **81**, 3684 (1984).
[10] M. W. Finnis and J. E. Sinclair, Philo. Mag. A. **50**, 45 (1984).
[11] A. P. Sutton and J. Chen, Philo. Mag. Lett. **61**, 139 (1990).
[12] M. F. Horstemeyer, M. I. Baskes and S. J. Plimpton, Acta. Mater. **49**, 4363 (2001).
[13] J. M. Haile, *Molecular Dynamics Simulation, Elementary Methods* (Singapore: John Wiley & Sons, Inc., 1992).